AD-A031 713 MASSACHUSETTS INST OF TECH LEXINGTON LINCOLN LAB F/G 20/1
BGO REFLECTIVE-ARRAY COMPRESSOR (RAC) WITH 125 MICROSECONDS OF --ETC(U)
SEP 75 V S DOLAT, R C WILLIAMSON F19628-73-C-0002
UNCLASSIFIED MS-4090 ESD-TR-76-261 NL

1 OF 1
AD
A031713

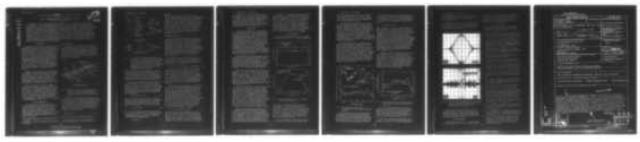

END

DATE
FILMED
12-76

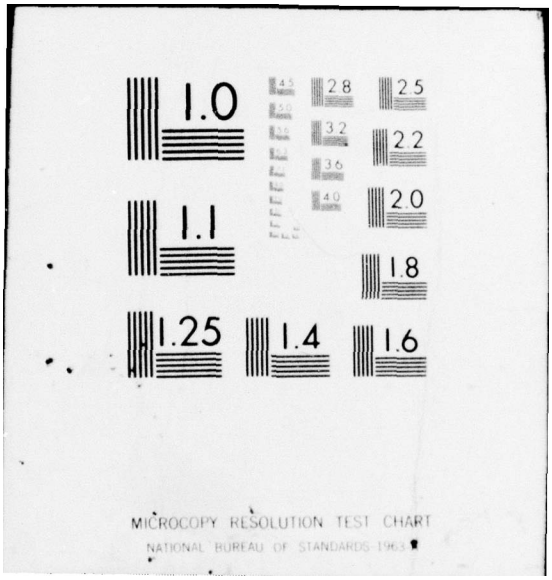
1.0
1.1
1.25
1.4
1.6
2.8
2.5
3.2
2.2
3.6
2.0
4.0
1.8
MICROCOPY RESOLUTION TEST CHART
NATIONAL BUREAU OF STANDARDS 1963

ESD-TR-76-261

AD A031713

BGO REFLECTIVE-ARRAY COMPRESSOR (RAC) WITH 125 μs OF DISPERSION*

V. S. Dolat and R. C. Williamson
Lincoln Laboratory, Massachusetts Institute of Technology
Lexington, Massachusetts 02173

ABSTRACT. Linear FM pulse expanders and compressors in the reflective-array configuration have been fabricated on bismuth germanium oxide substrates. The low surface-wave velocity on this material and the folded RAC configuration allow 125 μs of dispersion over the 2.5-MHz bandwidth to be obtained in a compact device. The reflective arrays were depth weighted to provide a flat frequency response in the down-chirp expansion lines and a Hamming frequency response in the up-chirp compression lines. Maximum amplitude deviation from ideal was 0.5 dB. Midband (60 MHz) insertion loss was approximately 33 dB in both types of devices. Reflective arrays ion-beam etched with 500-eV argon ions showed no evidence of surface alteration or anomalous acoustic propagation loss. Phase compensation with Au-on-Cr films yielded a typical residual phase error of 2.0°, and sidelobes below 33 dB were obtained in a subsystem comprising an expander, compressor, and associated electronics. Successful development of the devices depended on solving problems of angular accuracy of the reflective arrays and temperature sensitivity. These problems are especially severe in devices with small fractional bandwidth and large dispersion.

Introduction

A compact pulse-expansion and compression subsystem was developed for an experimental airborne radar. Sensitivity requirements dictated that the transmitted waveform be relatively long (125 μs). Because of its low surface-wave velocity, bismuth germanium oxide (BGO) is an attractive substrate material on which to fabricate a device for processing a waveform of this duration. Low velocity combined with foreshortening advantages of the folded reflective-array-compressor (RAC) configuration[1,2] yield devices which easily fit on commercially available 15-cm substrates. The use of BGO as a substrate material for RAC devices is new. It is generally considered a difficult material to use and success in this development required that difficulties associated with material non-uniformity, metal adhesion, bonding, and ion-beam etching be solved.

Simplicity and compactness of the pulse-expansion and compression subsystem was obtained by operating at the radar IF (60 MHz) and by developing expanders and compressors with conjugate chirp slopes. These features allowed for the complete elimination of mixers and oscillators from the subsystem. Also, Hamming weighting for sidelobe suppression was incorporated in the compression lines. This avoided the necessity of an external weighting filter.

Because the output of the pulse compressor is processed by a relatively slow digital system, the bandwidth of the expansion and compression lines was set at 2.5 MHz. This bandwidth yields a relatively small fractional bandwidth, which, combined with large dispersion, imposes especially tight specifications on pattern accuracy, alignment and temperature control. In addition, there exists a fundamental limit on the degree to which a RAC device can be phase compensated[3,4]. This limitation is more severe in small-time-bandwidth devices.

Design Considerations

The devices described herein use reflection gratings whose periodicity varies quite slowly as a function of position. Because of this, a small change in reflector characteristics such as that caused by temperature change or angular rotation, causes the effective center of reflection at any given frequency to shift by a large amount. For this reason, angular alignment and temperature must be carefully controlled.

* This work was sponsored by the Department of the Air Force.
1975 Ultrasonics Symposium Proceedings, IEEE Cat. #75 CHO 994-4SU

Angular Alignment

The familiar RAC configuration is schematically illustrated in Fig. 1. The basic operation of this device has been described previously[1-3]. Angular alignment of the reflection gratings relative to each other and relative to the transducers is critical[2]. For the crystal cut employed here, waves reflected at 90° have the same velocity as the incident wave and, accordingly, the reflectors must be placed at 45° relative to the transducers.

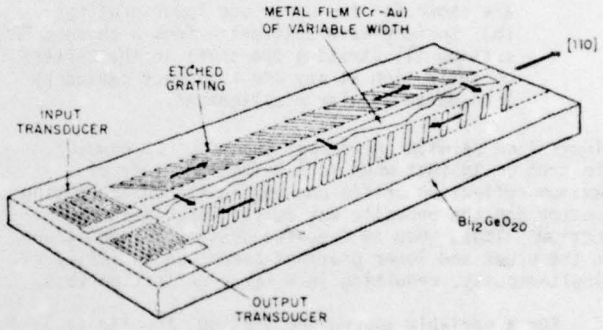

PHASE-COMPENSATED RAC

Fig. 1 Schematic diagram of reflective-array compressor. The metal film between the ion-beam etched gratings provides phase compensation by selectively slowing the surface wave.

Of the many possible angular errors, the most troublesome for the device described herein is illustrated in Fig. 2a. Here it is assumed that the gratings are correctly aligned at 90° relative to each other, but that there exists a transducer misalignment error $\delta\theta$. The resulting scattering vector diagrams are shown in Fig. 2a. For periodic gratings, the frequency of reflection will be a function of $\delta\theta$. For an angle of incidence of approximately 45°,

$$\frac{\delta f}{f} = \pm \delta\theta \,, \qquad (1)$$

where δf is the shift in frequency of reflection.

If the gratings form a corner reflector as shown, the wavefronts of the reflected waves will

This reprint may be reproduced to satisfy needs of U. S. Government agencies.

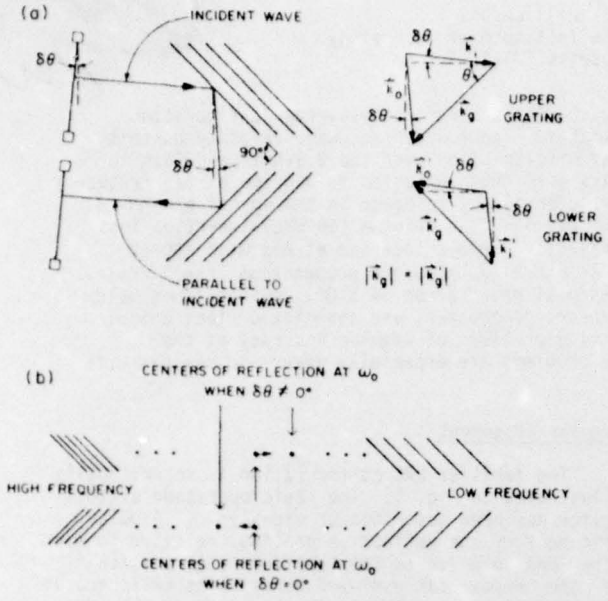

Fig. 2 (a) Geometry of surface-wave reflection from a periodic grating with transducers misaligned by an angle δθ. The scattering-vector diagrams are shown for the upper and lower gratings. (b) Surface-wave scattering from a chirped RAC grating illustrating the shift in the centers of reflection at any one frequency caused by transducer angular misalignment.

always line up with the output transducer. However, the problem is that when $\delta\theta \neq 0$ the frequency of maximum reflection shifts one way in the upper grating section and the opposite way in the lower grating section. Thus, when $\delta\theta \neq 0$, the scattering conditions in the upper and lower gratings cannot be satisfied simultaneously, resulting in a large reflection loss.

For a variably spaced RAC grating, the limits on $\delta\theta$ can be established in terms of the chirp parameters. Figure 2b illustrates this situation. At a particular frequency, there is a certain position in the grating, referred to as the center of reflection, at which the scattering condition is satisfied. In addition, one can define a number of effective reflectors N_e that are predominantly contributing to the reflection at any one frequency[3,5]

$$N_e = (T\Delta f/2)^{1/2}\, f/\Delta f, \tag{2}$$

where T is the chirp dispersion and Δf is the chirp bandwidth. When $\delta\theta$ changes, the centers of reflection for the upper and lower gratings shift in opposite directions, and the number ΔN of the grating lines over which the centers of reflection shift is given by

$$\Delta N = f_o T\, \delta f/2\Delta f, \tag{3}$$

where δf is the frequency shift caused by rotation. If ΔN is large in comparison to N_e, the wave reflected by the upper grating will "miss" the effective reflecting section of the lower grating. Equations (1)-(3) yield the limitation on $\delta\theta$;

$$\delta\theta << (2N_e)^{-1}. \tag{4}$$

This limitation is particularly severe when N_e is large or equivalently, when a device has a combination of small fractional bandwidth and large time-bandwidth product. For the device described herein, $N_e = 300$ reflectors at center frequency. Relation (4) implies $\delta\theta << 0.1°$. An angular error corresponding to $\delta\theta \approx 0.1°$ occured during generation of the first photomask used for the BGO devices. A device fabricated with this mask exhibited an excess reflection loss of more than 10 dB. It was necessary to obtain an accurately aligned mask and to maintain alignment within 0.02° in order to achieve the desired reflection loss in subsequent devices.

Temperature Dependence

Of the three most commonly used substrates for surface wave devices, BGO has the largest temperature coefficient of delay γ[6,7]. In order to adequately stabilize the response of the RAC devices, provisions were made to thermostat the devices at 60°C. A change from room temperature to 60°C corresponds to a downward shift of 0.31 MHz in the midband frequency of each device, representing 12% of the total bandwidth. These shifts had to be taken into account with designing the transducer and grating masks. Measured temperature dependence of the devices indicated a value γ equal to 138×10^{-6}/°C which compares well with previous data[6].

In a small fractional bandwidth device, the delay of the compressed pulse is a strong function of temperature and is equal to the group delay τ_o at center frequency f_o. The temperature induced change in group delay $\delta\tau_o$ is given by[8]

$$\delta\tau_o = [1 \pm f_o T/\Delta f \tau_o]\gamma\tau_o .(\text{change in temperature}) \tag{5}$$

The plus sign is for a device with an up-chirp impulse response and the minus sign is for a down-chirp device. For most dispersive devices, T is slightly larger than $2\tau_o$. Thus for small-fractional-bandwidth devices, the largest term in the brackets in (5) is approximately equal to $2f_o/\Delta f$. Correspondingly, the temperature sensitivity of a dispersive device is "amplified" by a factor approximately equal to $2f_o/\Delta f$. This sensitivity is most troublesome in devices with small fractional bandwidth and large dispersion.

For the devices described herein, it was necessary to stabilize the delay to the compressed pulse to within ±60 ns. This implies that if one device of a pair of expansion and compression lines is held at constant temperature, the temperature variation of the other device could be no more than ±0.16°C. This degree of temperature control is difficult to achieve in an operational environment. However, if the expansion and compression lines are placed in the same oven, with both devices held at the same temperature, the variation of total delay through the cascaded devices will be the sum of the variations given by (5). The large positive and negative terms cancel, provided that the devices are identical except for the sign of the chirp slope. In this case, the overall temperature variation is given by

$$\delta\tau_o = 2\gamma\tau_o .(\text{change in temperature}). \tag{6}$$

Equation (6) implies that a temperature control of ±1.5°C is required. Commercially available ovens can easily achieve this stability over a wide range of ambients. Thus it is possible to meet the specifications of temperature stability, provided that a pair of expansion and compression lines are in good thermal contact with each other and mounted in the same oven.

In addition to stabilizing the delay to the compressed pulse, it is also necessary to stabilize temperature in order to maintain a match between the chirp slopes of the expansion and compression lines, and to assure that the amplitude weighting of the compression line remain symmetrical about f_0. However, these variations place much less stringent requirements on temperature stability than those imposed by stabilizing the overall delay.

Fabrication

The RAC devices schematically illustrated in Fig. 1 were fabricated on 001-110 cut BGO substrates which are fifteen cm long. These substrates had to be selected with some care. Boules from which BGO surface-wave plates are fashioned contain a core structure along the growth axis. This core can be distinguished from the rest of the material by its darker appearance. RAC devices that were fabricated on substrates wherein this core came close to the surface exhibited a drastically degraded response and excessive insertion loss. Electrostatic probe[9] measurements of surface waves on cored material indicated that the cored region had a slower velocity than the normal material and that material nonuniformities caused a drastic distortion of the surface-wave beam. All devices fabricated on core-free substrates achieved near-theoretical response.

For bombardment with a neutralized beam of 500 eV argon ions, the etching rate was measured to be 13.5 angstroms/sec at a flux density of 4×10^{15} ions/cm^2 (0.65 ma/cm^2 prior to the neutralization). No anomalous damage, change in stoichiometry, or increased attenuation was observed with BGO surfaces. Thus, it was not necessary to ion etch in a partial pressure of oxygen or to perform any post-etching surface treatments, as is the case with $LiNbO_3$ surfaces.[2,10,12]

Grooves were ion-beam etched to depths of approximately 0.1 μm or 0.35% of a wavelength at the center frequency. At the beginning of this development, the reflection coefficient γ_{90} for 90° reflection from a vertical step was unknown. A model of device reflection loss[5,13] fitted the measured device response provided that $\gamma_{90} = 0.23\ h/\lambda$. Overall reflection loss was ~18 dB at center frequency. Depth weighting[10,11] was employed to yield a flat amplitude response for the expansion lines and Hamming-weighted amplitude response for the compression lines.

A transducer beamwidth of 3.48 mm (125 wavelengths at f_0) was chosen to minimize diffraction effects. Calculations of surface wave diffraction[14] show that significant amplitude ripples (and associated phase ripples) occur for normalized diffraction distances greater than 0.2. The transducer aperture was chosen to keep the normalized diffraction distances less than this value for the longest delays encountered. Wider apertures would require more substrate area and more precise alignment. A twelve-finger-pair transducer with this aperture has a radiation impedance of 110 ohms and can be approximately matched to a 50-ohm load by simple inductive tuning to yield a nearly flat response and a total conversion loss of only 10.5 dB for the input and output transducers combined.

Because of the poor adhesion of thin metal films to BGO, particular attention to metallization and bonding was required. Metallization consisting of 0.3 μm of Au over 0.03 μm of Cu yielded adequate, but not outstanding, adhesion[15]. Of the several bonding methods attempted, ultrasonic bonding of hard Au wire using a wedge tip[15] provided the highest yield (80%) of reliable bonds. After ultrasonic bonding, the bonds were strengthened with the addition of small dots of conductive epoxy around the wire-pad interface.

Following initial fabrication, the phase response of the devices was tested and phase compensation patterns were generated and metallized in the region between the gratings, see Fig. 1. The metallization for phase compensation consisted of 0.045 μm of Au over 0.03 μm of Cr. Calculations[16] indicate that for this ratio of metal thicknesses, the velocity in the metallized region is relatively independent of absolute metal thickness provided the thickness is small in comparison to a wavelength. Following phase compensation, a slot was cut between the transducers to provide feedthrough isolation. The finished device is mounted and sealed in a brass package.

Device Performance

The CW frequency responses of the pulse expander and compressor are shown in Fig. 3a and 3b, respectively.

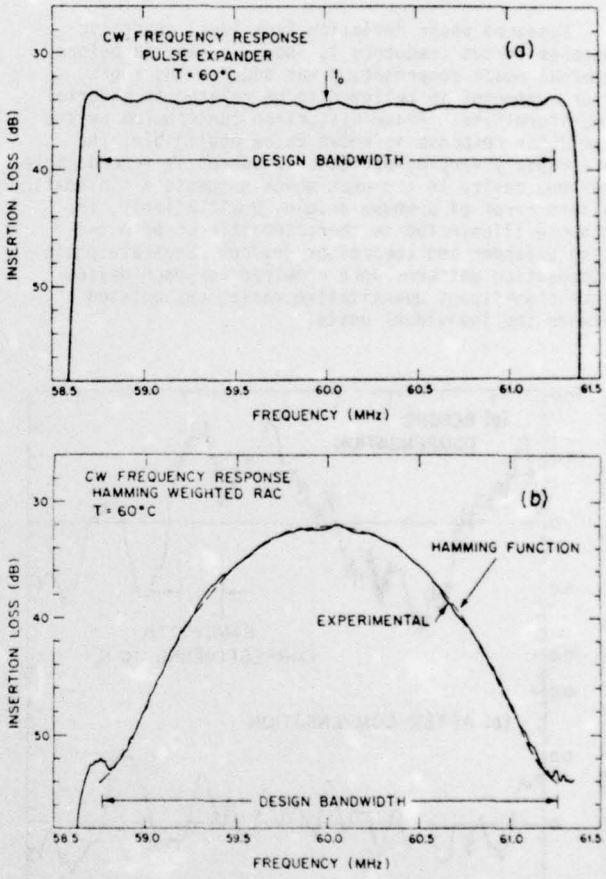

Fig. 3 Frequency Responses of (a) pulse expander, and (b) pulse compressor.

In each case the response is centered at 60.0 MHz when operated at the design temperature of 60°C. Total midband CW insertion loss is typically 33 dB with a 1 dB variation among devices. The series-tuned transducers contribute 10.5 dB loss; propagation and diffraction losses amount to -4.5 dB; and the grating reflection loss contributes the remaining -18 dB to the total. The Hamming-weighted compression lines exhibit a maximum deviation from an ideal Hamming function of approximately 0.5 dB.

Direct electromagnetic feedthrough was reduced to a level more than 100 dB below the input signals

by placing a metal septum in the slot between the input and output transducers, by using an indium gasket between the septum and cover-plate assembly, and by carefully orienting the tuning inductors to minimize electromagnetic coupling.

Large Fresnel amplitude and phase ripple occur near the band edges of a RAC device in which the grating is abruptly terminated. In order to avoid excessive ripple and thus more easily evaluate device response, tapered tails were added to the impulse response of the RAC devices by adding more grooves to the gratings. Total dispersion of the extended grating was 150 μs over a 3 MHz bandwidth. The extended impulse response was terminated gradually by ion-beam etching the "tail" sections with a cosinusoidal depth-weighting function. When this is done, the ideal phase response is very close to a simple quadratic variation versus frequency.

Measured phase deviation from ideal quadratic response versus frequency is shown in Fig. 4a before internal phase compensation was added. The cubic error component is believed to be related to material nonuniformities. Phase distortion contributed by the transducer response is known to be negligible. The more rapidly varying periodic component is reproducible from one device to the next which suggests a systematic pattern error of unknown origin. Qualitatively, the response illustrated is characteristic of both the pulse expander and compressor devices. Separate phase-compensation patterns were required for each device since significant quantitative variations existed between the individual units.

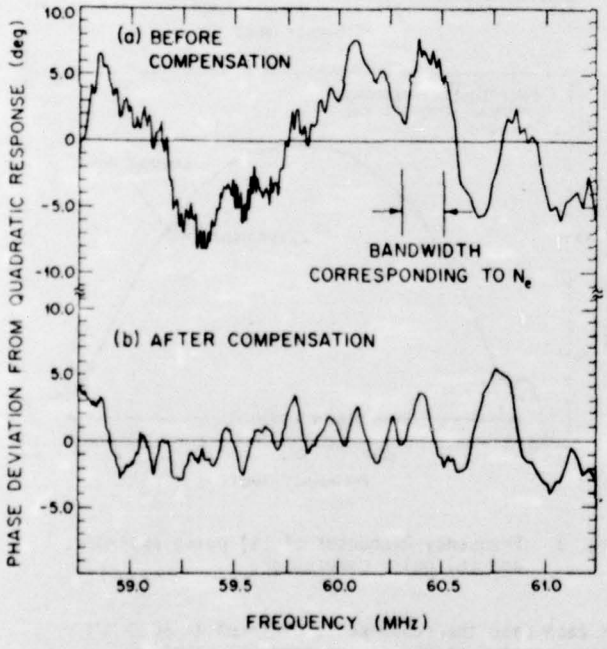

Fig. 4 Phase response of a RAC device (a) before and (b) after internal phase compensation.

Device phase response following internal phase compensation is shown in Fig. 4b. Only the cubic error component was successfully compensated. The ability to phase compensate RAC devices is based on the premise that a given position in the reflective grating corresponds to one particular frequency and that the width of the phase compensation at that given position affects the phase response only at that frequency. A measure as to the extent that this is true can be obtained from a consideration of the fractional part of the entire grating contributing to reflections at any one frequency. This fraction is given by

$$N_e/N = (2/T\Delta f)^{1/2} \qquad (7)$$

Thus, one observes, that for small-time-bandwidth-product devices, a significant fraction of the grating contributes to the reflection at any one frequency, and it becomes increasingly less accurate to associate a given position in the grating with a particular frequency. The extent of N_e for this device is indicated in Fig. 4. The measured phase response is the result of the average contribution from an extended region in the grating, and the rapid variations in the width of the phase-compensation pattern are averaged over an extended region to yield a net effect on the phase which is relatively insensitive to the rapid variations. Thus it is difficult to compensate phase errors in RAC devices when those phase errors are more rapidly varying than a rate corresponding to $(T\Delta f/2)^{\frac{1}{2}}$ cycles across the passband. This is the result observed in Fig. 4.

The metal overlay pattern was also used to align the dispersion slope of all devices to the same value. Before compensation, the individual chirp slopes varied by as much as 1% among the seven devices fabricated during this development program. Measured phase deviation from ideal linear response versus frequency for a cascade of an expander and compressor is shown in Fig. 5. The absence of a significant quadratic component in the phase response of the cascaded devices indicates that the chirp slopes of the individual units are well matched.

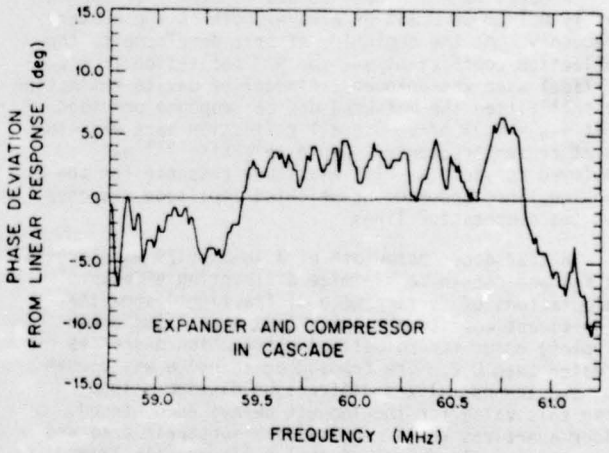

Fig. 5 Measured phase deviation from ideal linear response for a pulse expander and compressor in cascade.

The pulse expansion and compression lines were tested in a pulse compression circuit. An impulse applied to the expansion line was obtained by gating a 60.0 MHz carrier to provide a 200 ns impulse (12 cycles). The expanded pulse was gated over the central 125 μs interval, with no limiting, before the signal was applied to the compression lines.

Typical pulse compression performance is shown in Fig. 6. Both devices were operated at 60°C in the component oven assembly. The -3dB and -30dB widths

of the compressed pulse are 0.53 μs and 1.22 μs, respectively. The values obtained are those expected for a 2.5 MHz bandwidth device which is Hamming amplitude weighted.

The shoulder on the main lobe shown in Fig. 6b is approximately -33dB below the peak compressed pulse level. The remaining sidelobes at -35dB and below are consistent with the measured periodic phase and amplitude errors in the devices.

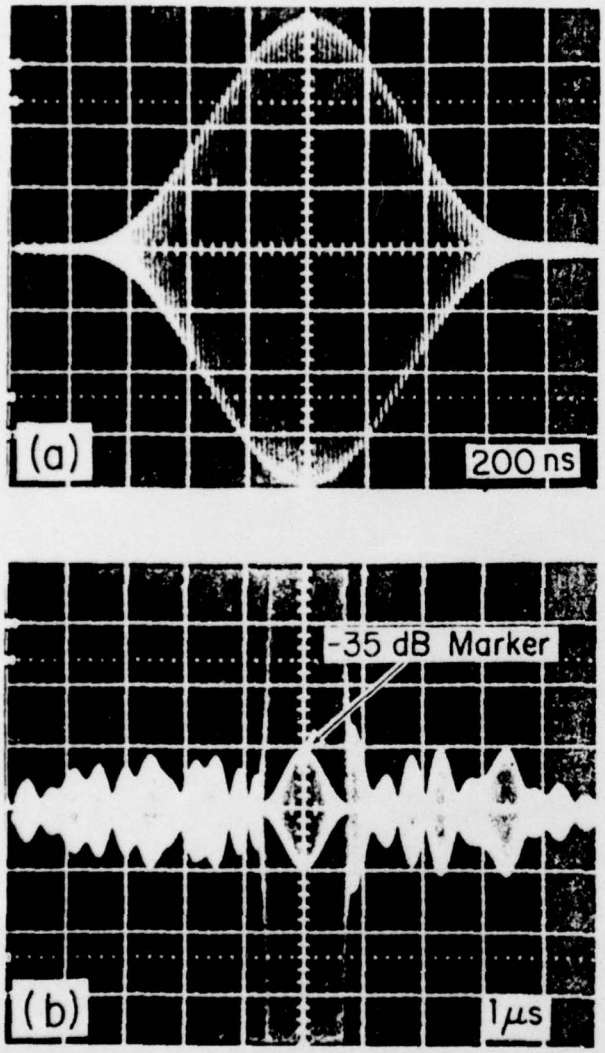

Fig. 6 (a) Main lobe of compressed pulse. (b) Double exposure of compressed pulse showing the sidelobe structure with 35 dB difference in attenuation between exposures.

These results indicate that BGO is a practical material for RAC devices and is particularly useful when large dispersion is required. With proper care, problems of alignment, material nonuniformity, metal adhesion, and temperature sensitivity can be solved to yield high-performance devices.

Acknowledgements

The authors are indebted to H. I. Smith who oversaw device fabrication, to N. Efremow and W. Kernan who did the photolithography and metallization, and to W. Brogan and R. Eager who did the ion-beam etching. J. Alusow and L. Grant designed the packages and accomplished the difficult task of bonding. R. Konieczka assembled the devices and S. Cupoli and J. Holtham evaluated their performance.

References

1. R. C. Williamson and H. I. Smith, "Large-time-bandwidth-product surface-wave pulse compressor employing reflective gratings", Electron. Lett., vol. 8., pp. 401-402, Aug. 1972.
2. R. C. Williamson and H. I. Smith, "The use of surface elastic-wave reflection gratings in large time-bandwidth pulse-compression filters", IEEE Trans. Microwave Theory Tech., vol. MTT-21, pp. 195-206, Apr. 197.
3. R. C. Williamson, "Large-time-bandwidth-product devices achieved through the use of surface-acoustic-wave reflection gratings", Proceedings of International Specialists Seminar on Component Performance and System Applications of Surface Acoustic Wave Devices, London: IEE, 1973, pp. 181-190.
4. R. C. Williamson, V. S. Dolat, and H.I. Smith, "L-Band reflective-array compressor with a compression ratio of 5120", 1973 Ultrasonics Symposium Proceedin New York: IEEE, 1973, pp. 490-493.
5. R. C. Williamson, "Reflection-grating devices", in Surface-Wave Devices, H. Matthews, Ed, New York: Wiley, to be published, Chapter 9.
6. P. C. Meyers and M. B. Schulz, "Temperature effects in reflective surface-acoustic-wave delay lines", Electron. Lett., vol. 9, pp. 523-525, Nov. 1973.
7. A. J. Slobodnik, Jr., "A review of material tradeoffs in the design of acoustic surface wave devices at UHF and microwave frequencies", IEEE Trans. Sonics Ultrasonics, vol. SU-20, pp. 315-323, Oct. 1973.
8. T. A Martin and M. B. Schulz, private communication.
9. R. C. Williamson, "Improved electrostatic probe for measurement of elastic surface waves", IEEE Trans. Sonics Ultrasonics, vol. SU-19, pp. 436-441, Oct. 1972.
10. H. I. Smith, J. Melngailis, R. C. Williamson, and W. T. Brogan, "Ion-beam etching of surface gratings", 1973 Ultrasonics Symposium Proceedings, New York: IEEE, 1973, pp. 558-563.
11. H. I. Smith, "Fabrication techniques for surface-acoustic-wave and thin-film optical devices", Proc. IEEE, vol. 62, pp. 1361-1387, Oct. 1974.
12. H. L. Garvin, and R. D. Weglein, "The effect of ion-beam sputtering on acoustic surface wave propagation" 1972 Ultrasonics Symposium Proceedings, New York: IEEE, 1972, pp. 190-193. These results which indicate no surface alteration of $LiNbO_3$ after 500-eV argon ion bombardment disagrees with our result.
13. T. A. Martin, "The IMCON pulse compression filter and its applications", IEEE Trans. Microwave Theory Tech. vol. MTT-21, pp. 186-194, Apr. 1973.
14. T. L. Szabo and A. J. Slobodnik, Jr., "The effect of diffraction on the design of acoustic surface wave devices", IEEE Trans. Sonics Ultrasonics, vol. SU-20 pp. 240-251, July 1973.
15. A. J. Slobodnik, Jr., W. J. Kearns, J. H. Silva, and T. E. Fenstermacher,"A comparison of SAW wrap-around delay line geometries", 1974 Ultrasonics Symposium Proceedings, New York: IEEE, 1974, pp. 185-188.
16. L. P. Solie, "Surface acoustic wave velocities for two metal layers on lithium niobate and bismuth germanium oxide substrates", IEEE Trans. Sonics Ultrasonics, vol. SU-20, pp. 379-382, Oct. 1973. Calculations for the 001 cut were provided by private communication.

UNCLASSIFIED

SECURITY CLASSIFICATION OF THIS PAGE (When Data Entered)

REPORT DOCUMENTATION PAGE		READ INSTRUCTIONS BEFORE COMPLETING FORM
1. REPORT NUMBER (18) (19) ESD-TR-76-261	2. GOVT ACCESSION NO.	3. RECIPIENT'S CATALOG NUMBER
4. TITLE (and Subtitle) (6) BGO Reflective-Array Compressor (RAC) with 125 μs of Dispersion. → micro seconds		5. TYPE OF REPORT & PERIOD COVERED (9) Journal Article,
		6. PERFORMING ORG. REPORT NUMBER (14) MS-4090
7. AUTHOR(s) (10) ~~Dolat~~, Victor S. Dolat Williamson, Richard C. Williamson		8. CONTRACT OR GRANT NUMBER(s) (15) F19628-73-C-0002
9. PERFORMING ORGANIZATION NAME AND ADDRESS Lincoln Laboratory, M.I.T. P. O. Box 73 Lexington, MA 02173		10. PROGRAM ELEMENT, PROJECT, TASK AREA & WORK UNIT NUMBERS 649L
11. CONTROLLING OFFICE NAME AND ADDRESS Air Force Systems Command, USAF Andrews AFB Washington, DC 20331		12. REPORT DATE (11) 22 Sep[illegible]75
		13. NUMBER OF PAGES 5 (12) 6p.
14. MONITORING AGENCY NAME & ADDRESS (if different from Controlling Office) Electronic Systems Division Hanscom Air Force Base Bedford, MA 01730		15. SECURITY CLASS. (of this report) UNCLASSIFIED
		15a. DECLASSIFICATION DOWNGRADING SCHEDULE n/a

16. DISTRIBUTION STATEMENT (of this Report)

Approved for public release; distribution unlimited.

17. DISTRIBUTION STATEMENT (of the abstract entered in Block 20, if different from Report)

18. SUPPLEMENTARY NOTES

1975 Ultrasonics Symposium Proceedings, IEEE Cat. #75, CHO 994-4SU

19. KEY WORDS (Continue on reverse side if necessary and identify by block number)

Reflective-array compressor Bismuth germanium oxide Phase-compensation

20. ABSTRACT (Continue on reverse side if necessary and identify by block number)

Linear FM pulse expanders and compressors in the reflective-array configuration have been fabricated on bismuth germanium oxide substrates. The low surface-wave velocity on this material and the folded RAC configuration allow 125 μs of dispersion over the 2.5-MHz bandwidth to be obtained in a compact device. The reflective arrays were depth weighted to provide a flat frequency response in the down-chirp expansion lines and a Hamming frequency response in the up-chirp compression lines. Maximum amplitude deviation from ideal was 0.5 dB. Midband (60 MHz) insertion loss was approximately 33 dB in both types of devices. Reflective arrays ion-beam etched with 500-eV argon ions showed no evidence of surface alteration or anomalous acoustic propagation loss. Phase compensation with Au-on-Cr films yielded a typical residual phase error of 2.0°, and sidelobes below 33 dB were obtained in a subsystem comprising an expander, compressor, and associated electronics. Successful development of the devices depended on solving problems of angular accuracy of the reflective arrays and temperature sensitivity. These problems are especially severe in devices with small fractional bandwidth and large dispersion.

microseconds

degree

207650

DDC RECEIVED NOV 5 1976

DD FORM 1 JAN 73 1473 EDITION OF 1 NOV 65 IS OBSOLETE

UNCLASSIFIED

SECURITY CLASSIFICATION OF THIS PAGE (When Data Entered)